BOND LINE CHARACTERISTICS OF NEW EDGE CONNECTIONS OF CROSS-LAMINATED TIMBER IN THE WEAK DIRECTION BASED ON MILLED PROFILED CONNECTION PLATES FROM LAMINATED VENEER LUMBER MADE OF BEECH

KLEBFUGENEIGENSCHAFTEN VON NEUEN BRETTSPERRHOLZ-VERBINDUNGEN IN DER NEBENTRAG-RICHTUNG MITTELS PROFILIERT GEFRÄSTER ANSCHLUSSPLATTEN AUS BUCHEN-FURNIERSCHICHTHOLZ

Marian Claus, Cristóbal Tapia, Simon Aicher

Materials Testing Institute (MPA), University of Stuttgart, Otto-Graf-Institute

SUMMARY

The paper reports on the manufacturing and bond-line characteristics of a new screw glued edge connection for the secondary direction of cross-laminated timber (CLT) plates. The connection principle consists of laminated veneer lumber (LVL) plates made of beech wood with milled finger joint-like profiles bonded into form-fitting cavities of the jointed CLT plates. Two alternatives, A and B, of 2D- or 3D-shaped finger profiles were investigated, requiring either a three-axis CNC or four-axis (robotic) milling. The cramping pressure for the joint manufacture was applied by screw gluing in combination with a modified gap-filling two-component polyurethane adhesive. The investigations on the local bond line thickness and shear strength were performed at two joints of large-scale bending specimens, loaded to failure and reported separately, where the joints have not suffered any evident damage.

For the post-mortem investigations the joints were cut into several cross-sectional slabs, then further subdivided at specific locations into small block shear specimens. The visual and microscopic inspection revealed prevailingly no obvious bond line deficiencies. Except hereof is a larger ($\approx$ 27 cm^2) interface void with a gap of about 3 mm not filled with adhesive. The bond line thickness, with a mean value of 0.14 mm and a coefficient of variation (COV) of about 40%, was found to be quite evenly distributed over the bond surfaces, i.e. no evident trend in the spatial distribution was observed. The mean shear strengths of the wide side finger

joint bonded areas, oriented *quasi* parallel to the CLT plane, of about 11 MPa were almost equal for both connection alternatives A and B. However, alternative B, with tapered finger faces, presented a higher scatter with a COV of 18% vs. 12% for alternative A. The mean shear strength of the vertical finger surfaces of alternative A reached a mean value of 11.4 MPa, excluding two miss-bonded outliers. The higher COV of 20% as compared to the wide bond line faces is owed to the smaller size of the shear planes, enforced by the connection geometry.

The results indicate that the overall bonding quality of the newly developed connection principle well supports the intended joint use. However, a deeper understanding of the cause of observed adherend/bond line voids is needed in order to improve the manufacturing process and to further increase the reliability of the developed connections.

ZUSAMMENFASSUNG

Der Beitrag berichtet über die Herstellung und die Klebfugeneigenschaften einer mittels Schraubenpressklebung hergestellten Verbindung von Brettsperrholz (BSP)- Platten in der Nebentragrichtung. Die Verbindung besteht aus Einlegeplatten aus Furnierschichtholz (FSH) aus Buche mit eingefrästen Keilzinkenprofilen, die in passgenaue Aussparungen auf der Ober- und Unterseite der zu verbindenden Brettsperrholzplatten eingeklebt werden. Es wurden zwei 2D- bzw. 3D-geformte Keilzinkenprofil-Varianten, A und B, untersucht, deren Herstellung eine drei-Achs (CNC) bzw. eine (robotische) vier-Achsbearbeitung erfordert. Der Pressdruck für die Herstellung der Verbindung wurde unter Verwendung eines modifizierten fugenfüllenden Zwei-Komponenten Polyurethanklebstoffs mittels Schraubenpressklebung aufgebracht. Die Untersuchungen zu lokalen Klebfugendicken und zu Scherfestigkeiten wurden an zwei Verbindungen von großformatigen bis zum Bruch geprüften Bauteilen durchgeführt, wobei die Verbindungen in den Traglastversuchen, über die getrennt berichtet wird, augenscheinlich unbeschädigt blieben.

Für die Post-Mortem-Untersuchungen wurden die Verbindungen in mehrere Querschnittsscheiben geschnitten, die sodann an speziellen Stellen in kleine Blockscherprüfkörper aufgetrennt wurden. Die visuellen und mikroskopischen Inspektionen ergaben überwiegend keine offensichtlichen Klebfugenbeeinträchtigungen. Eine Ausnahme hiervon ist ein größerer (rd. 27 cm^2) Fugenhohlraum mit einer Klaffung von rd. 3 mm, der nicht mit Klebstoff verfüllt war. Die Klebfugendicke mit einem Mittelwert und Variationskoeffizienten (V) von 0.14 mm

bzw. 40% war bei allen Klebeflächen gleichmäßig verteilt, d.h. es war kein Trend in der räumlichen Verteilung festzustellen. Die mittleren Scherfestigkeiten der breiten, (quasi) parallel zur Elementebene angeordneten Keilzinkenfinger-Klebeflächen von rd. 11 MPa waren für beide Verbindungsalternativen nahezu gleich. Die Alternative B mit der geneigten Keilzinkenoberfläche wies jedoch eine größere Streuung (V = 18%) im Vergleich zur Alternative A mit V = 12% auf. Die mittlere Scherfestigkeit der vertikalen Keilzinkenfinger-Oberflächen der Verbindungsalternative A betrug bei Ausschluss zweier fehlverklebter Ausreißer 11.4 MPa. Der im Vergleich zu den horizontalen Klebeflächen größere Variationskoeffizient von 20% ist der kleineren Größe der Scherflächen geschuldet, die sich aus der Verbindungsgeometrie ergeben.

Die Ergebnisse zeigen, dass die Verklebungsqualität der neuentwickelten Verbindungen für den vorgesehenen Einsatz in genereller Hinsicht zufriedenstellend ist. Unabhängig hiervon, ist jedoch ein vertieftes Verständnis für die Ursachen der festgestellten Fügeteil/Klebfugen-Klaffungen erforderlich, um den Herstellablauf zu verbessern und die Zuverlässigkeit der entwickelten Verbindungen weiter zu erhöhen.

1. INTRODUCTION

The advancing climate change and current sustainability and resource efficiency issues have triggered fundamental discussions within the building sector, mostly summarized in the concepts of efficiency (materials and processes) and reduction of CO_2 emissions. In this context, timber structures have received a fair amount of attention owed to their positive environmental characteristics and high performant mechanical properties. Especially in the field of multi-storey buildings, an increased interest has surged, marked by a high research output and rapid development of new solutions, where cross-laminated timber (CLT) plays a major role. Due to their high degree of prefabrication and comparatively fast on-site assembly CLT panels have become a widespread construction element in wooden high-rise buildings. Regarding floor elements, a pending major challenge is posed by the connection of the individual prefabricated plates to achieve a bidirectional load-bearing floor element, allowing for a higher flexibility in the floor plan layout and column arrangement.

Contributions to these efforts have been presented e.g. by Loebus et al. [7], Kawrza et al. [6] and Asselstine et al. [1]. As part of the Cluster of Excellence “Integrative Computational Design and Construction for Architecture (IntCDC),”

at the University of Stuttgart and granted by the German Ministry of Science, the Research Project 3 (RP3) deals with the development of multi-story timber construction systems with a strong emphasis on the implementation of computational design and automated manufacturing processes. In the course of this project a concept for a robotically manufactured, bending-stiff glued edge connection for the secondary direction of CLT floor panels was developed and investigated [2]. The connection (see Fig. 1) is based on two specially milled laminated veneer lumber (LVL) plates glued onto the complementary-milled outer secondary layers of the jointed CLT plates (more details below), thus relying exclusively on the glued surfaces for the load transfer. The connection was tested in four- and three-point bending tests in order to examine its resistance to bending and a combination of bending and shear, respectively, and to validate the accuracy of the developed analytical and finite element models.

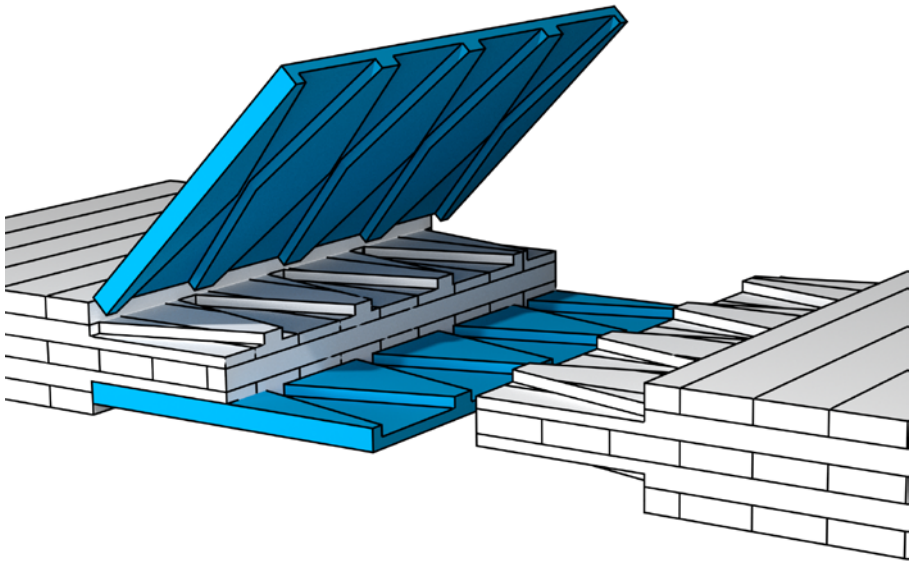

Fig. 1: Developed edge connection concept for the secondary direction of CLT plates

The combination of an absolute reliance on the load transfer through the glued interface and a rather complex-shaped joint geometry elevates the issue of allowable geometric tolerances to the highest priority. To ensure a high strength and long-term integrity of the glued joints, the geometric complexity of the connection requires a high degree of manufacturing accuracy and a precise joining/bonding process. In this paper, the overall quality and mechanical properties of the glued interface of the manufactured connection prototypes are examined in detail. Here, only the prototypes tested under a combination of shear and bending load were investigated. In order to analyze the quality of the glued interface, the connection is cut transversely in cross-sectional slabs of 5 cm width, which are then inspected visually under a digital stereo-microscope in order to assess the glueline thickness.

Thereafter, the slabs are further subdivided into small block shear specimens in order to evaluate the bond strengths by means of block shear tests. From the mechanical properties of the glued interface and its quality, conclusions about the feasibility and challenges associated with the developed glued CLT connection are drawn.

2. DESCRIPTION OF CONNECTION

The newly developed edge connection for CLT plates consists of two specially milled beech LVL plates glued onto the complementary-milled profiles of the outermost secondary layers of both connecting CLT plates, i.e. the layers oriented in the secondary load-bearing direction of the plate (see Fig. 1). For the case of a five-layer CLT plate, these two layers are responsible for the resistance of practically 100% of the bending moment in the secondary direction, and are therefore the only layers that need to be connected. For the case of a seven-layer CLT plate, this premise still holds, as the small contribution of the central layer is negligible.

The base geometry at the interface between CLT and LVL resembles a finger-joint, which serves to increase the total bonding area due to the additional vertical surfaces, allowing for a more efficient transfer of shear stresses (see Fig. 1). This pattern is repeated a total of n times to obtain the final connection geometry.

The sketched concept was investigated with two alternative geometries, illustrated in Figs. 2a and b. For the case of alternative A (Fig. 2a) all joint surfaces are arranged either horizontally or vertically. In order to reduce stress concentrations observed at the ends of the connection in preliminary finite element (FE) simulations, alternative B (Fig. 2b) was developed. This alternative considers a tapered wide-side finger surface in the length direction of the connection in order to gradually transfer the load and reduce stress concentrations by around 8% as compared to alternative A. The details of the manufacturing process are given below.

Fig. 3 depicts the intended use of the developed connection to join two long span CLT plates in the secondary load bearing direction. As can be seen, rather than having a single, continuous connection, a series of discrete, shorter joints segments are conceived. This is mainly related to the difficulty of maintaining the allowed tolerances as the joint length increases. In contrast, shorter connection elements are more manageable and easier to manufacture. Furthermore, constraints due to the maximum dimensions of the produced LVL plates must be considered.

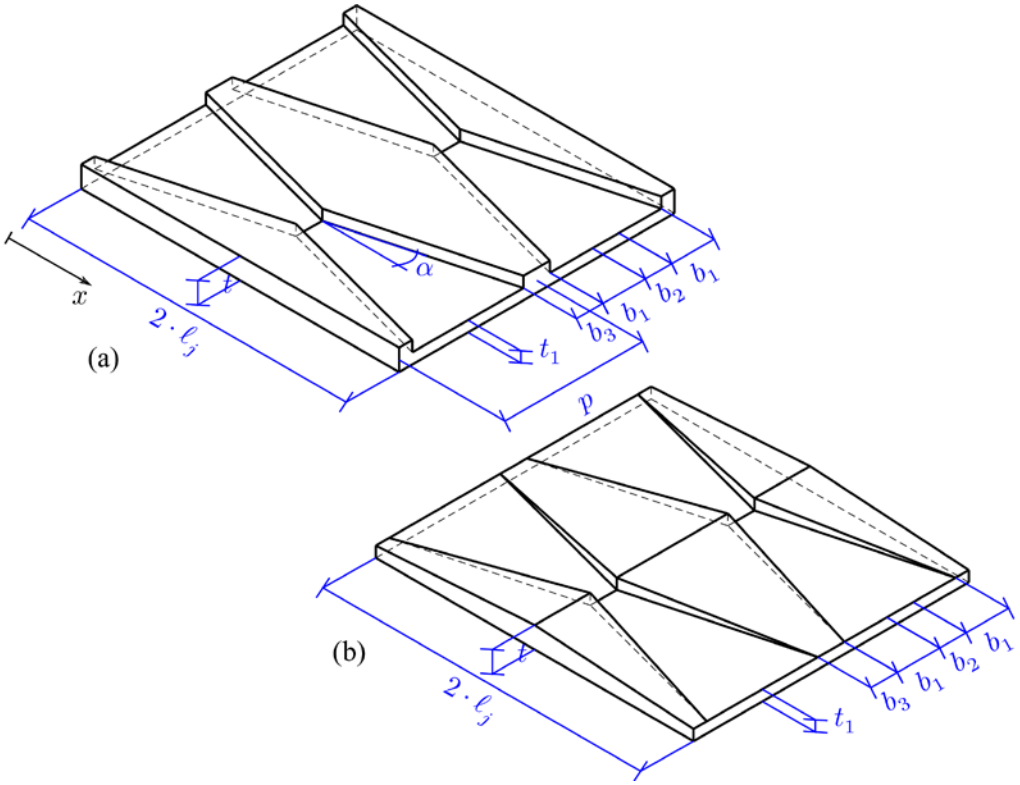

Fig. 2: Geometry and dimensional notation of the LVL connecting plates of the studied joint configurations. (a) alternative A, (b) alternative B

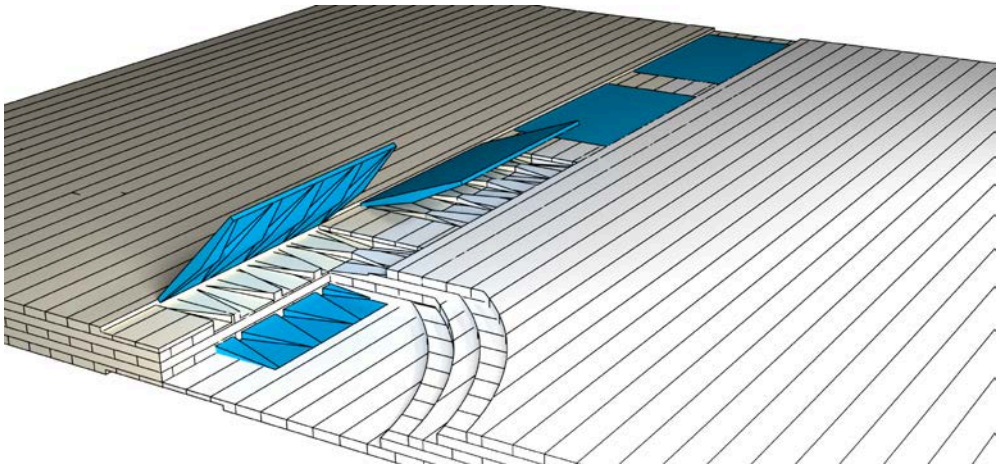

Fig. 3: Application of the connection concept for joining two CLT plate elements in the secondary load bearing direction

3. MANUFACTURE OF SPECIMENS

3.1 Geometry of studied configurations

For the experiments four specimens were manufactured and tested, consisting of two specimens of each alternative A and B. For both alternatives the joint region was tested either under a pure bending moment or under a mixed shear-moment load configuration. The specimens consisted of two five-layer CLT strips with a cross-section (depth × width) of 200 mm × 580 mm aligned and jointed in their

weak direction. The specific dimensions defining the geometry of the LVL plates and the bonding interfaces of the connection are presented in Table 1 (see also Fig. 2a and b).

Table 1: Dimensions of the profiled LVL jointing plates (for variable definition see Fig. 2)

ℓ_j	p	α	b_1	b_2	b_3	t_1	t_2	n
[mm]	[mm]	[°]	[mm]	[mm]	[mm]	[mm]	[mm]	[–]
250	140	9.1	40	40	20	20	20	4

3.2 Milling of connection elements

Due to the differences in the geometries of alternatives A and B, two different approaches were used for the milling of the CLT and LVL plates. In the case of alternative A, whose geometry consists exclusively of vertical and horizontal faces, a three axis CNC milling machine was used. For the case of alternative B, however, owed to the inclined wide finger surfaces, a machine with an additional degree of freedom is needed, in this case, a robotic arm. Following, the two milling processes are described.

For the CNC-milling of the components of alternative A, a CNC machine of type "Pro-Master 7017," company Holzher GmbH, was used. The milling was performed at the Institute for Machine Tools (IfW), University of Stuttgart, in a collaboration with the Materials Testing Institute (MPA), University of Stuttgart. The following milling tools were used: an end mill cutter for the bulk material of the top-most layer, a roughing cutter (Ø=20 mm) for the finger-joint region, and a finishing cutter (Ø=20 mm) to ensure a clean surface.

The CLT plates were positioned with the help of locating pads on one side of the CLT and were then fixed by means of screw clamps. To achieve the needed precision in the positioning of the elements, firstly the lateral sides of the CLT in the region of the connection were milled to obtain a total width of exactly 580 mm. This ensures a precise positioning when turning the CLT plate to mill the opposite side, as the geometries at both sides must match exactly. The milling of the LVL counterparts was performed with the same machine. The procedure is simpler than for the CLT plates, as the LVL elements are milled only on one side. Vacuum clamps were used to secure the elements.

The more complex geometry of alternative B was milled with a robotic arm of type “KR 420 R3080,” company Kuka AG, enabling a total of six degrees of freedom. The milling and related preparation work was performed at the Institute of Computational Design (ICD), University of Stuttgart, in collaboration with MPA.

Firstly, each plate was placed vertically on its narrow, long edge and fixed in this position. This allows for the robot to mill both wide sides without moving the plate, hence constituting a noteworthy advantage as compared to the CNC milling process used for alternative A.

The LVL counterparts were fixed by means of four screws on the milling-opposite side, and were processed in two steps. Firstly, the inclined surface contour was milled, and in a second step the finger joint-like cavities were produced. Fig. 4 shows the milled CLT surface of joint alternative B all together with the second step of the connection assembly.

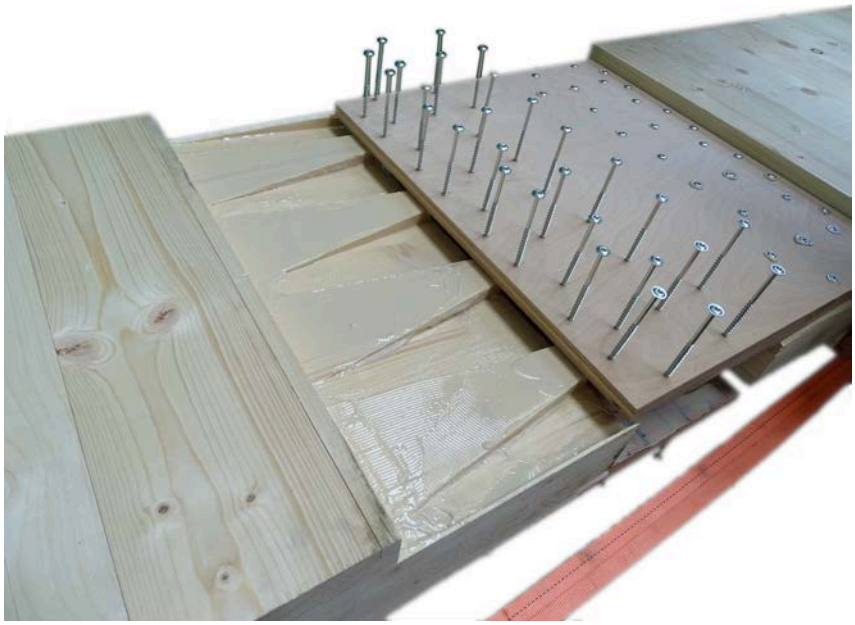

Fig. 4: View of profiles CLT surfaces of connection alternative B and second step of joint assembly by screw gluing

3.3 Assembly of connection

For the gluing of the LVL plates onto the CLT elements, a gap-filling, fiber reinforced two-component polyurethane adhesive from the producer Henkel AG was used. The adhesive represents an adequately modified prototype version of an adhesive being certified for thick bond line operations for glued-in rods and screw gluing. The application of the required cramping pressure was performed by means of partially threaded, self-tapping screws, according to a predefined pattern.

The connections were assembled in two steps: firstly, each LVL plate was screw-glued onto one of the CLT plates. Then, both preasembled halves were jointed by screw-gluing. A total of 800 g/m² of adhesive was spread single-sided onto the surfaces by means of a profiled spattle. The employed self-tapping partially threaded screws with a washer type head (diameter d_h = 13.6 mm) according to ETA-12/0114 [5] had a nominal diameter of 6 mm, a total length of 100 mm and a threaded length of 60 mm. Due to the rather complex profile topology of the bond areas, a rather dense arrangement of screws was chosen in order to achieve best possible gap closures, where the actual cramping pressure was of secondary interest in view of the gap-filling adhesive. The chosen screws are characterized by a characteristic head pull-through parameter of $f_{\mathrm{head},k}$ = 14.4 MPa. Hence, the maximum characteristic cramping force which can be exerted by the screw results in $F_{\mathrm{head},k} = 14.4 \cdot 13.6^2$ = 9.9 kN. In total $n = 26$ screws were used for each of the four bonded joint areas, i.e. the total cramping force amounted to $F_{\mathrm{press},k}$ = 257 kN. The mean cramping force can be assumed as minimally $1.1 \cdot F_{\mathrm{press},k}$, so 280 kN. This results in a rough estimation of the mean nominal cramping pressure of $F_{\mathrm{press,mean}}/A_{\mathrm{joint}}$ = 280 kN / (580 mm × 250 mm) = 1.9 MPa. In a more detailed manner, considering a radial pressure spread with an angle of 45° from the screw head periphery, the nominal pressure influence areas of the screws are: 2650 mm² at 20 mm depth (upper LVL layer) and 6880 mm² at 40 mm depth (lower LVL layer). This results in very high local mean pressures per screw of $(9.9 \times 10^3 \cdot 1.1)/2652\ (6880)$ = 4.4 MPa (1.4 MPa).

4. MEASUREMENT OF BOND LINE THICKNESS OF GLUED LVL-CLT INTERFACE

To analyze the visual quality of the bond line the connection was cut in a first step transversely along four sections (I-IV) defined in Figs. 5 and 6 for alternatives A and B, respectively, resulting in cross-sectional slabs having the full height of the joint and a thickness of 50 mm parallel to the element's length (sawing blade thickness ≈ 5 mm). After a general visual assessment and the recording of clearly recognizable bond gaps, the quality of the glued joint and the bond line thickness distribution were examined more closely by means of a digital stereomicroscope (Olympus, SZX2-ILLT) connected to a computer. The bond line thickness was recorded for each cross-section at more or less regular intervals of 1 cm with the

help of the software Olympus Stream Essentials v 2.4.3. In the following, the horizontal glued surfaces of alternative A, as well as the horizontal and inclined surfaces of alternative B are termed “wide surfaces.”

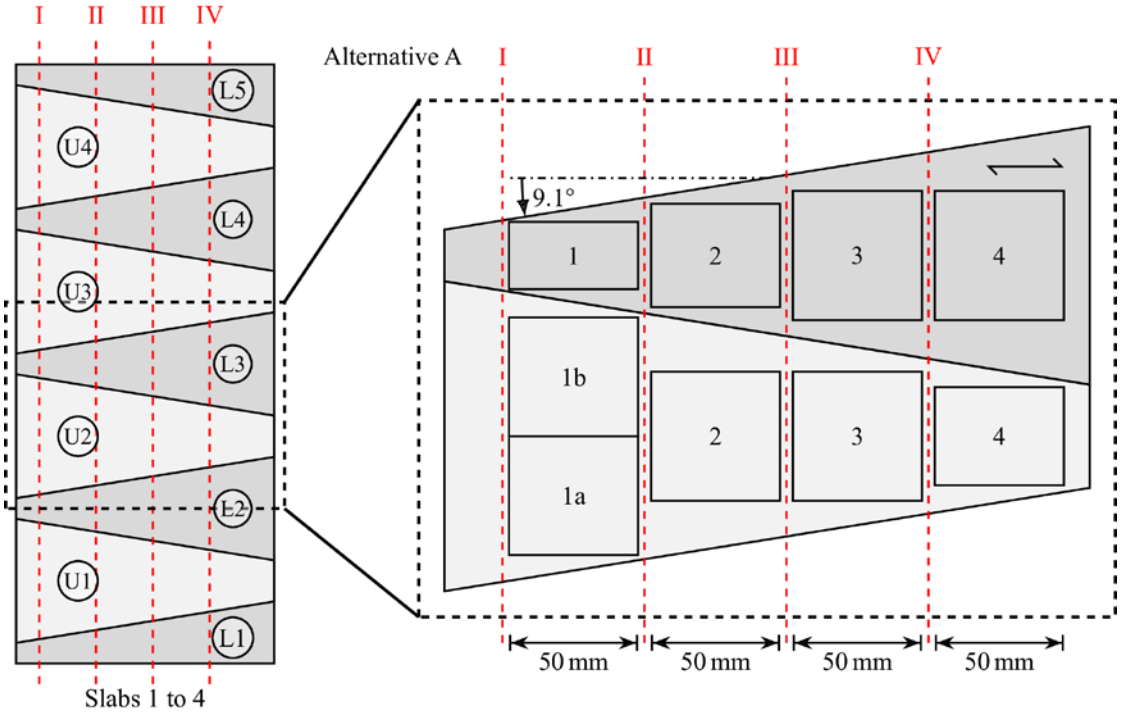

Fig. 5: Location and numbering of block shear test specimens for alternative A (for explanations on Ui, Li see below; Cross-section C-C addressed in Fig. 9)

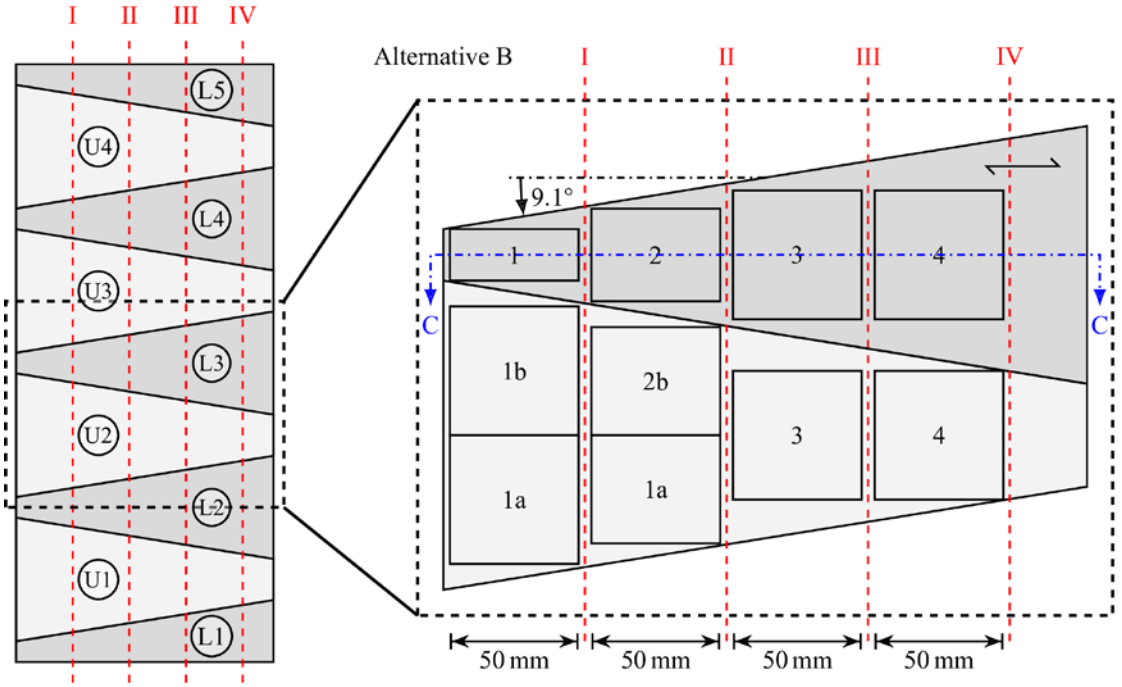

Fig. 6: Location and numbering of block shear test specimens for alternative B (for explanations on Ui, Li see below)

5. SHEAR TESTS OF THE GLUED SURFACES

The shear strength of the bonded interfaces was evaluated by tests with small block shear specimens measuring 50 mm in the shear direction. Figs. 5 and 6 reveal the specimen cutting pattern for alternatives A and B, respectively. Fig. 7 exemplary shows a selection of some of the block shear specimens, comprising the bond lines of both (compression and tension side) LVL adherends glued onto the CLT plate. The elements were divided into three different specimen types: horizontal upper faces of the finger joints (Ui) and horizontal (or inclined) lower faces (Li) according to Figs. 5 and 6 (wide surfaces), and vertical faces according to Fig. 8. Depending on the specimen type, i.e. on their location, the wood fibers form an angle with the bonding surfaces (vertical surfaces and specimens Li of connection alternative B). The effect of these differences on the shear strength of the specimens will be addressed below.

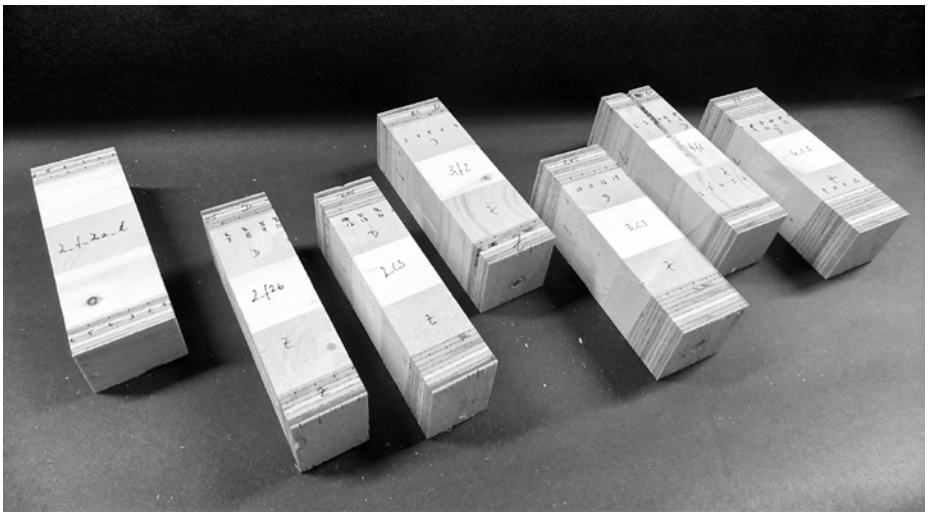

Fig. 7: Shear block specimens for the testing of horizontal surfaces, cut from alternative B

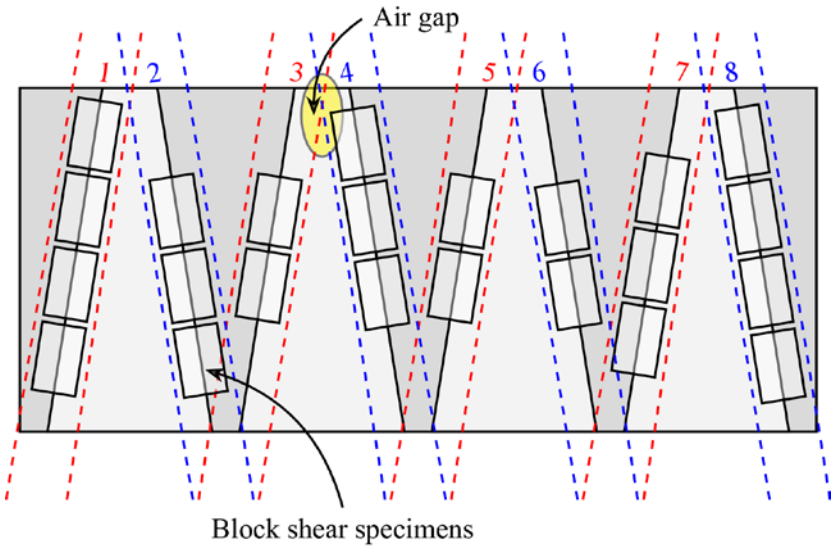

Fig. 8: Definition of block shear test specimens of the vertical surfaces for alternative A

For the case of alternative B (Fig. 6) only the wide finger surfaces were examined. In order to test the specimens obtained from the inclined wide bond line surfaces of alternative B in pure shear, the specimen endgrain faces, i.e. the oppositely located shear force application areas had to be cut perpendicular to the bond surface. This ensures that the load and bond line coincide. Fig. 9 shows the above discussed sawing principle of the specimens.

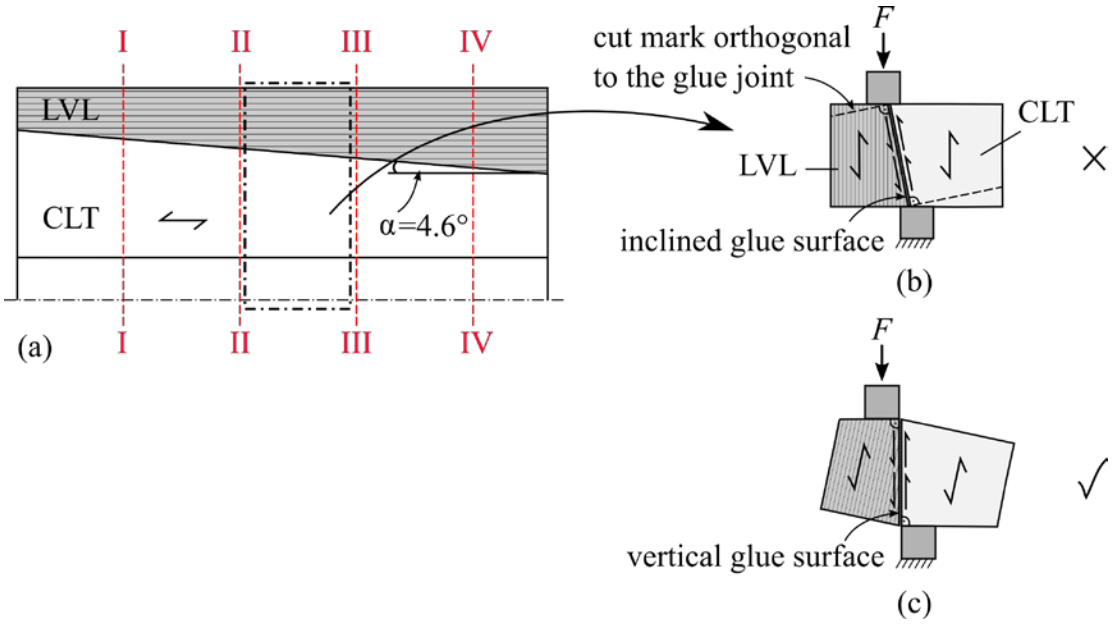

Fig. 9: Cutting scheme of block shear specimens of the vertical bond lines; (a) lateral view on cut C–C (see Fig. 6) (b) primary cutting shape (c) final specimen shape with co-linear vertical load and shear planes

6. RESULTS OF VISUAL AND MACROSCOPIC INVESTIGATIONS

6.1 General assessment of bond quality

In a first visual assessment of the bond lines, visible at both endgrain faces of cross-sectional slabs 1 to 4, and further at all four faces of the block shear specimens, the vast majority of the bond lines did not show apparent signs of bonding anomalies. There was, however, one case where a major unbonded gap between the LVL and CLT surface was observed (see Figs. 10a and b). The reason for this large air gap could not be clearly identified, but must be related to some error during the milling process. The observed gap, filled only to a minor extent by the gap-filling adhesive, measures about 3 mm in thickness and 66 mm in length and 40 mm width (rd. 27 cm^2). In general, it can be noted that discontinuities are rare and that the overall view of the bond is very good.

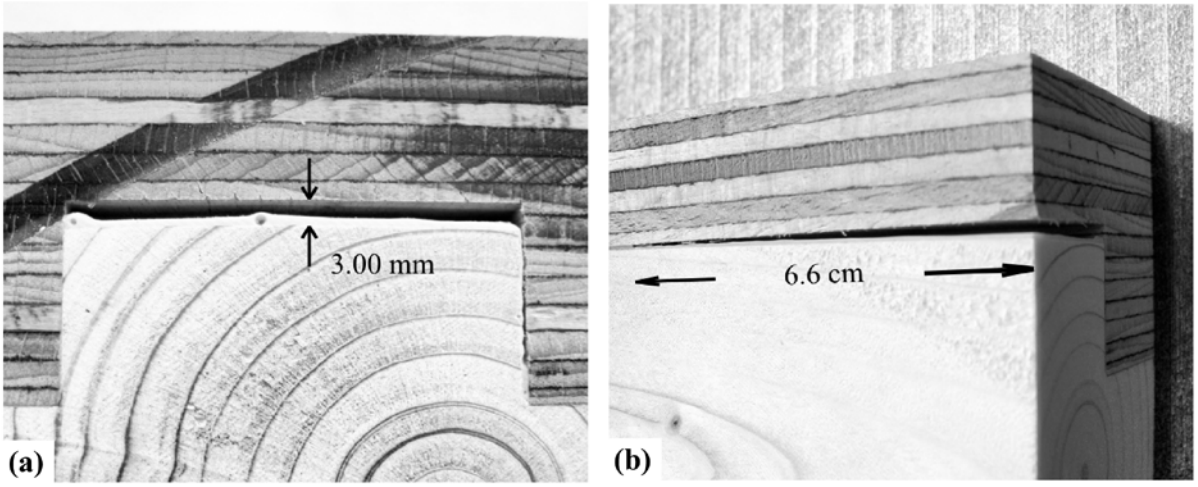

Fig. 10: Bond line gap observed at end grain face in specimen of alternative A (see Fig. 8); (a) frontal view of the cross-section (b) view on the longitudinal axis of the bond discontinuity

6.2 Distribution of thickness in the glued interface

Without optical magnification, a clearly uneven thickness distribution of the adhesive bond can be observed close to the base at cross-section I ($x \approx 50$ mm, see Fig. 2) area of the CLT finger joint of alternative A (see Fig. 11).

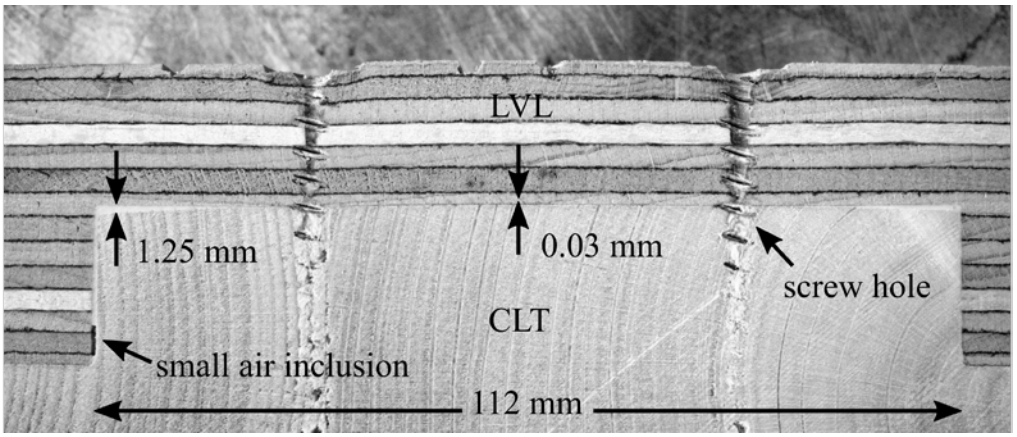

Fig. 11: View of bond line thickness variation in the end grain face of alternative A on cross-section I ($x = 50$)

In the immediate vicinity of the screws used to apply the required pressure the bond is apparently thinner as compared to the bond thickness at the edges of the finger-joint geometry. This characteristic can be attributed to the lower local stiffness of the LVL batten, measuring 20 mm in its thinner region, allowing for larger uneven deformations on the bond surface driven by the punctual very high pressure applied by the screws (rd. 4.4 MPa). Table 2 presents the thicknesses measured in the middle, t_{mid}, and on the edge, t_{edge}, of one finger-joint element, recorded on the four analyzed cross-sectional cuts (see Fig. 5). The measured values suggest that the difference between t_{mid} and t_{edge} reduces along the tapering of

the fingers. With the decreasing width of the milled LVL cutout, and the reducing influence area of the screw, the effect of the local deflection in the immediate screw vicinity is also diminished.

Table 2: Bond line thicknesses of the wide finger joint surfaces at four different cross-sectional cuts (I-IV) measured at the middle ($y = 0$) of the finger-joint (t_{mid}) and at the edge (t_{edge})

Cross-section	Finger width	t_{mid}	t_{edge}
	[mm]	[mm]	[mm]
I	112	0.03	1.25
II	94	0.06	1.10
III	77	0.05	0.73
IV	60	0.05	0.20

The bond line thicknesses measured at intervals of 1 cm on the analyzed cross-sections I-IV were post-processed and summarized in the form of contour plots for the wide bond surfaces of alternative B. A statistical summary of the bond line thickness of each individual surface and for all surfaces is presented in Table 3. Figs. 12a,b and 13a,b present the measured bond line thicknesses as contour plots for the upper and lower surfaces, respectively. These figures also indicate the position of the screws used for the screw-gluing and the position of the measurement points, marked with white crosses.

Table 3: Statistical summary of bond line thickness on each individual surface

Surface	Element side	n*)	Mean	Std.	Min.	Max.	COV
		[–]	[mm]	[mm]	[mm]	[mm]	[%]
U	Compression	50	0.14	0.06	0.05	0.32	40.4
	Tension	50	0.12	0.05	0.03	0.28	45.6
L	Compression	43	0.14	0.05	0.05	0.27	34.9
	Tension	43	0.14	0.06	0.06	0.29	40.8
All	All	186	0.14	0.06	0.03	0.32	41.2

*) n: number of measurements

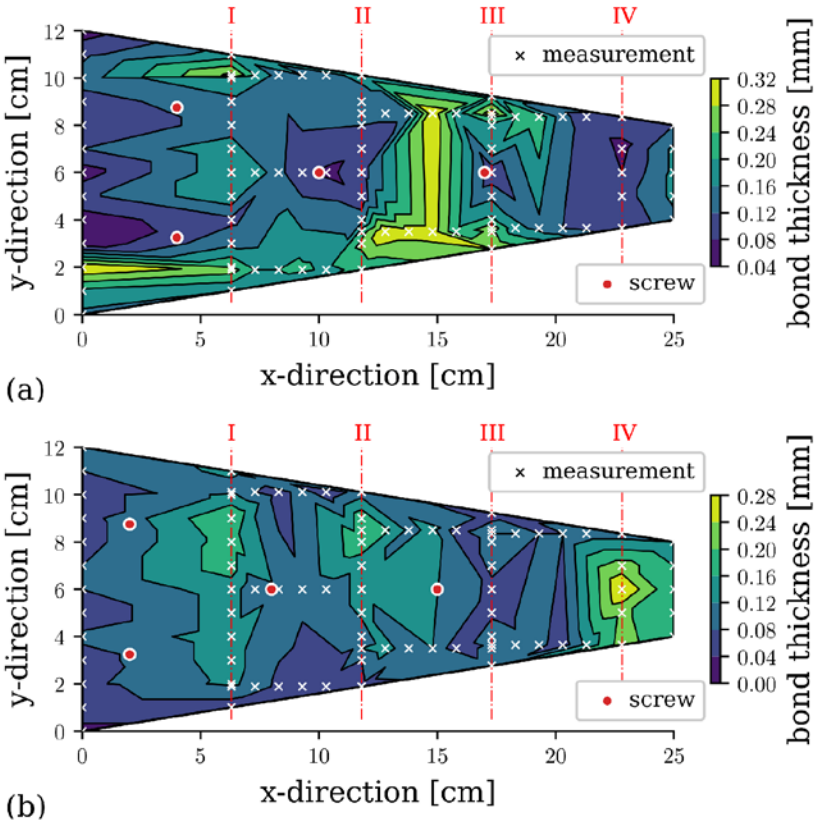

Fig. 12: Distribution of bond line thickness over the upper surfaces of alternative B (a) compression side (b) tension side

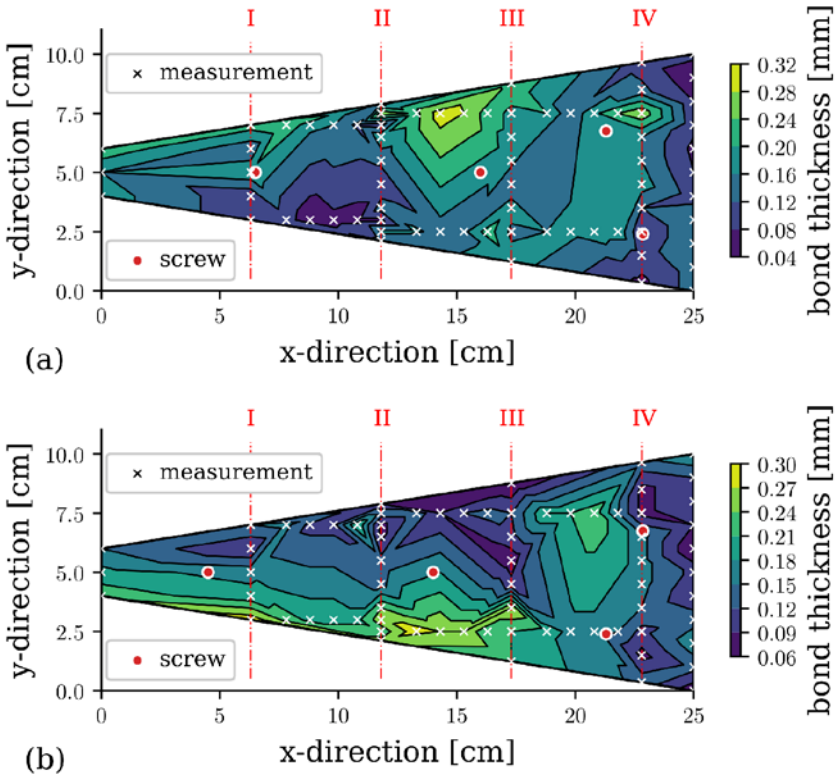

Fig. 13: Distribution of bond line thickness over the inclined surfaces of alternative B (a) compression side (b) tension side

Both Figs. 12a,b and 13a,b reveal a rather uniform distribution of the bond line thickness, where no clear distribution pattern can be stated. In fact, according to Table 3, the four investigated surfaces are characterized by rather equal mean and scatter values, with COVs in the range of 34% to 45%. Different to alternative A, an increase in bond line thickness towards the edges of the finger joint cannot be noted, which could be related to the slightly higher stiffness of the LVL connecting batten. This leads to the assumption, that if the stiffness of the joining elements is high, the bond thickness is mainly determined by the irregularities of the wood surface, which for the analyzed cases is well below 1 mm.

7. BLOCK SHEAR TEST RESULTS

7.1 Wide side finger surfaces

The results of the block shear tests are presented graphically for alternatives A and B in Figs. 14a,b and 16a,b. Table 4 presents a statistical summary of all results. In Figs. 14a and b the results are separated both by longitudinal location of the block shear specimens within the bond surface (positions 1–4, see e.g. Fig. 5) and by surface type (U: upper; L: lower, see e.g. Fig. 5). From Fig. 14a no clear trend in the development of strength can be observed, meaning that the bond quality is similar throughout the length (x-axis) of the connection for alternative A. For alternative B, Fig. 14b shows a moderately higher variation in general, with an average COV of 13.3% vs. 12.2% for connection A. Particularly noteworthy are the relatively low values of the inclined surfaces (L) at location 4 of alternative B (see Fig. 14b). For this case, the mean value of 7.5 MPa is 33% lower as compared to the mean shear strength of all other specimens. The fact that the fiber breakage of all specimens at location 4 was 100% indicates that the reduced shear strength is not consequence of a bonding issue. A visual inspection of these specimens—a subsample of which is presented in Fig. 15—clearly shows that the governing failure mode was rolling shear in one of the transverse layer of the LVL which happened to be located in the region of the bond line. Therefore, since the rolling shear strength is known to be significantly lower than the shear strength parallel to grain, the obtained lower values are well explained. Due to the local nature of this issue the influence on the overall strength of the joint is probably negligible. Nevertheless, an LVL plate without transverse layers should be considered for future developments, too, as this would eliminate any possible rolling shear related issues.

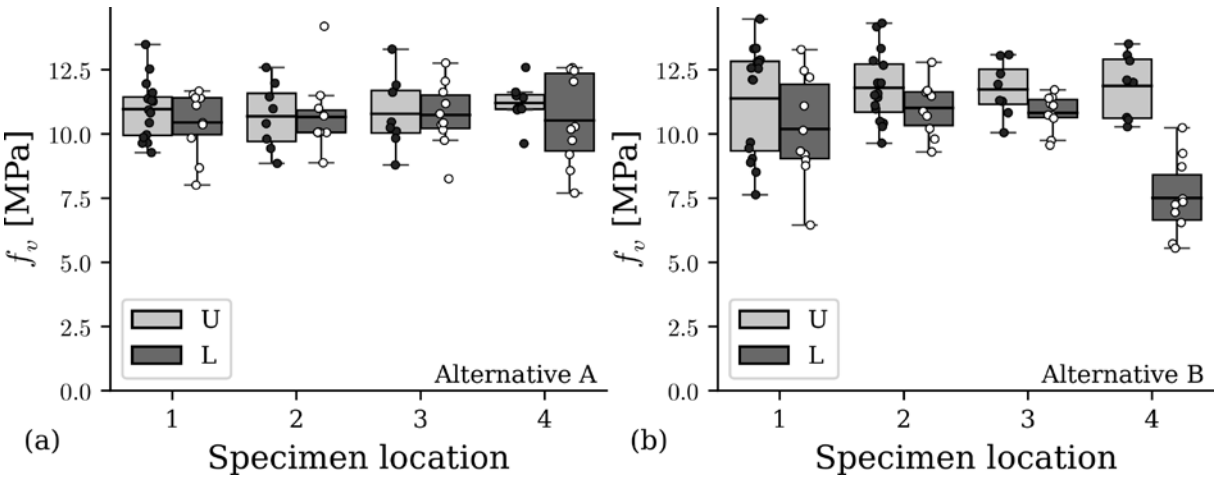

Fig. 14: Block shear strength results of wide finger surfaces (a) alternative A, (b) alternative B

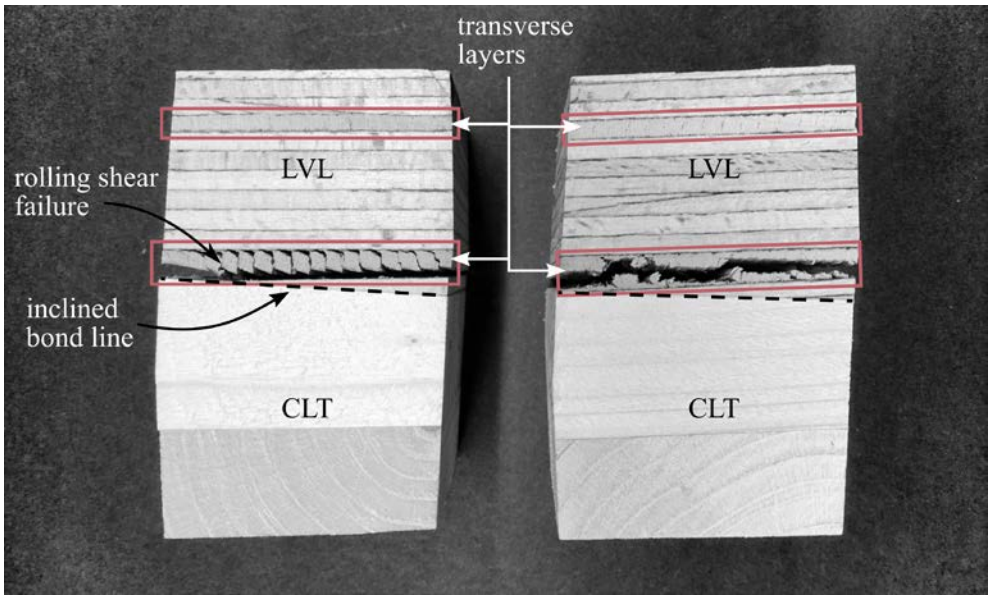

Fig. 15: Block shear specimens corresponding to the position 4 where low strength values were observed owed to rolling shear failure on the transverse layers of the LVL

Figs. 16a and b show the shear strengths grouped by each individual finger joint surface, Ui, Li, for alternatives A and B, respectively. The number of block shear specimens per surface ranges between four and six (see Figs. 5 and 6). The bond surfaces at both element sides of the connection are denoted as “compression” and “tension” sides, which should only be regarded as a descriptive label to differentiate both wide sides of the connection—i.e. no effect in strength is expected from the block shear specimens being on one side or the other. It can be seen that the strength variation within each finger joint bond surface is considerably smaller for alternative A as it is for alternative B, with their COVs being in average 9.6% and 17.4%, respectively. This results from the above observed fact of alternative B that the strength at the finger tip (position 4) is substantially lower than the

rest of the specimens at positions 1 to 3. The fact that this larger variation is observed at the tension side should not be considered as a consequence of damage induced during the previous testing of the connection. It is more likely that the observed lower strength values at the finger tip of alternative B is bound to tolerance/cramping pressure issues of the thin end of the finger with tapered thickness.

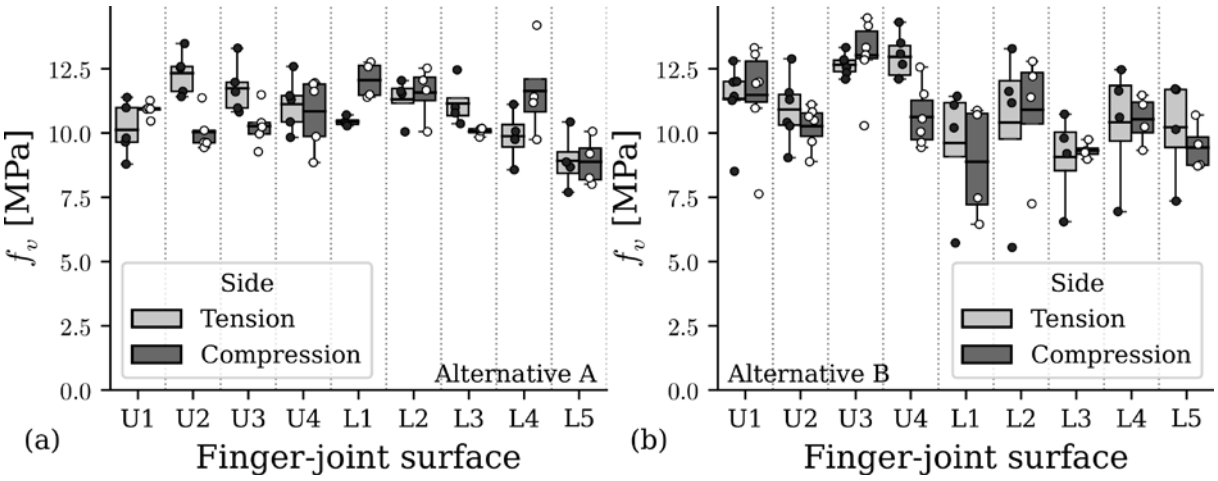

Fig. 16: Shear strength of block shear specimens separated by finger-joint surfaces (a) alternative A, (b) alternative B

Table 4 reveals that both alternatives A and B exhibit similarly high shear strengths on the mean level, varying between 9.9 MPa and 11.7 MPa. The major differences lay, as observed above, in the larger standard deviations of alternative B. In terms of standardized requirements, both the mean and individual values of the bond line shear strengths and the fiber breakage (FB) percentages meet the requirements according to EN 14080 [3] for block shear results of face-bonded GLT softwood laminations (see Table 5).

Table 4: Statistical summary of block shear strength results of different surfaces (wide and vertical) of connection alternatives A and B.

Alternative	Surface	n	Mean	Std.	COV	Min.	Max.	5%-quant.
		[–]	[MPa]	[MPa]	[%]	[MPa]	[MPa]	[MPa]
A	L	40	10.6	1.4	13.2	7.7	14.2	8.0
	U	40	10.9	1.1	10.5	8.8	13.5	8.8
	V	43	11.0	2.8	25.7	2.6	16.2	5.8
	L+U	80	10.8	1.3	11.9	7.7	14.2	8.5
B	L	40	9.9	2.0	20.0	5.6	13.3	6.3
	U	48	11.7	1.6	13.5	7.6	14.5	8.8
	L+U	88	10.9	2.0	18.2	5.6	14.5	7.4

U: upper wide side surfaces; L: lower wide side surfaces; V: vertical surfaces

The standard specifies that individual strength values must be > 6 MPa, except for the cases where FB = 100%, in which case the threshold is lowered to 4 MPa (this applies to alternative B, with a minimum value of 5.6 MPa). For shear strengths > 6 MPa, FB is a function of f_v, specified separately for individual $f_{v,\mathrm{mean}}$ values.

Table 5: Mean values of block shear strengths and fiber breakage (FB) of joint alternatives A and B, and requirements according to EN 14080 [3]

Surface	$f_{v,\mathrm{mean}}$	$\mathrm{FB}_{\mathrm{mean}}$	$\mathrm{FB}_{\mathrm{req.}}$
	[MPa]	[%]	[%]
A (L+U)	10.8	89	> 46
B (L+U)	10.9	94	> 46
A (V)	11.0	69	> 45

7.2 Narrow vertical finger surfaces

A statistical summary of the results of the vertical surfaces of connection A is presented in Table 4 (characteristic values computed for an assumed normal distribution according to EN 14358 [4]). The mean and standard deviation for all specimens is 11.0 MPa and 2.8 MPa, respectively. Different from the wide surfaces L and U two of the 43 specimens do not meet the requirements of EN 14080. The outliers and the extremely low minimum value of only 2.6 MPa are due to an almost absent bonding of the respective surfaces, probably owed to an uneven application of the adhesive on the vertical surfaces. Disregarding the extreme low values, the mean and standard deviation become 11.4 MPa and 2.3 MPa, respectively, with a minimum value of 7.6 MPa and a characteristic value of 7.2 MPa. It is worth noticing that the standard deviation remains rather high (COV = 20.2%) as compared to the wide finger surfaces discussed above. Considering the smaller testing area, limited to the height of 20 mm the finger-joints, any local bond discontinuity has a larger negative impact on the shear resistance as compared to the block shear specimens of the wide surfaces with a width of 50 mm, which explains the larger variation. The mean values of the vertical faces, shown in Table 4, meet the requirements of EN 14080.

8. DISCUSSION

The dissection of the new screw glued connection prototypes revealed that the bond quality is satisfactory for dry state conditions to a high degree. Only one large defect, denoted by a large air void with a gap of about 3 mm between the adherends, was found. Although this defect had no apparent effect in the global

resistance of the connection (reported separately), and no local damage was observed that could be attributed to it, the source of this kind of irregularities needs to be better understood. This is even more important as the joint profiles were CNC/robotically milled with identical machine setup. Both connections, A and B, analyzed here based on post-mortem dissections represent prototypes tested until failure under a mixed shear and moment loading. Finite element simulations have shown that for the case of a pure or prevailing moment loading, the shear stresses on the bond surfaces become even more relevant in relation to the overall capacity of the connection. Therefore, the observed defect could have a significant negative effect for such a loading scenario. Further analyses are needed in order to better understand the internal redundancy of connections of the investigated type in order to better assess the different parameters of the connection geometry and manufacturing process.

Although the vertical narrow finger surfaces have experienced little or no pressure during the curing process owed to the described assembly procedure, the strength values are as high as for the wide side finger surfaces, bonded with a nominal pressure of about 2 MPa. This reveals that the used two-component fiber-reinforced PU adhesive, the bond shear strength does not depend on the applied pressure, which can be expected for a gap-filling adhesive to a large extent. However, a lack or reduced pressure can lead to larger air voids/gaps when pronounced bond surface topology variations/discontinuities exist, which then might not be fully bridged by the adhesive. In essence, a gap-filling adhesive helps to reduce tolerances-induced fitting problems of complex form-fitting contours, however, the range in which this holds true is limited, and there is a balance between fabricability and required tolerances that needs to be carefully assessed.

9. CONCLUSIONS

This paper analyzed visually apparent bond line quality parameters such as bond line thickness, discontinuities and dry shear strength of two new screw glued edge connections for the weak direction of CLT plates. The finger joint-type connections rely on CNC/robotic milling of 2D/3D-shaped finger profiles in the CLT adherends and the LVL-based connecting plate inserts. Block shear specimens were sawn from prototypes previously tested under a combined shear and moment loading configuration, where the failure took place outside the connection region. The presented results enable the following conclusions:

- In vast majority the visual appearance of the bond line judged by bond line thickness and lack/presence of voids was found well suited for the intended use.
- The distribution of bond line thickness was rather similar for all analyzed surfaces with mean values of about 0.14 mm, all together with a high scatter denoted by a coefficient of variation of about 40%.
- The dry shear strength of the specimens proved to be on the upper range of strengths required by the softwood GLT standard EN 14080. All specimens, except for two cases (≤ 4%), met the standard criteria. The outliers were owed to evident local bond defects in the vertical finger bond areas.
- In terms of mean values, the shear strength results of the vertical surfaces are almost identical to those from the wide finger surfaces. However, the standard deviation is about twice as large as for the wide finger surfaces (2.8 MPa vs. 1.3 MPa). This difference can be explained partly by the narrower width of the specimens taken from the vertical surfaces, which is limited to 20 mm.
- The high dry shear strength values of the vertical bond surfaces support the decision of using a fiber-reinforced gap-filling adhesive for the developed connection which requires quasi zero cramping pressure, and thus helps to minimize possible problems with the tolerances.
- The durability, i.e. long-term integrity aspects of the regarded bond lines, to be checked by boil-water, re-drying, cyclic tests, were outside the scope of the reported investigations.

ACKNOWLEDGEMENTS

The presented ongoing research is partially supported by the Deutsche Forschungsgemeinschaft (DFG, German Research Foundation) under Germany's Excellence Strategy – EXC 2120/1 – 390831618. The manufacture of the connection prototypes was only made possible by the engaged support of colleagues from collaborating institutes of University of Stuttgart. Specifically, the authors would like to thank Dr. F. Amtsberg, Institute of Computational Design (ICD), University of Stuttgart, and Dr. M. Schneider, Institute of Machine Tools (IfW), for their engaged knowledgeable support at the manufacturing stages of the new joints.

DATA AVAILABILITY

Some or all data, models, or code generated or used during the study are available in a repository or online in accordance with funder data retention policies. (doi: 10.18419/darus-2153, Ref. [8])

REFERENCES

[1] ASSELSTINE, J.; LAM, F.; ZHANG, C.: New edge connection technology for cross laminated timber (CLT) floor slabs promoting two-way action. In: *Engineering Structures* vol. 233 (2021), p. 111777. doi: 10.1016/j.engstruct.2020.111777

[2] CLAUS, M.: *Bonded connections of cross laminated timber plates in the secondary axis using CNC/robotically moulded jointing battens from laminated veneer lumber*, Materials Testing Institute (MPA), University of Stuttgart, (in German), Master's Thesis, 2020

[3] EN 14080: *Timber structures – Glued laminated timber and glued solid timber – Requirements*. Brussels, Belgium : European Committee for Standardization, 2013

[4] EN 14358: *Timber structures – Calculation and verification of characteristic values*. Brussels, Belgium : European Committee for Standardization, 2016

[5] ETA-12/0114: *European Technical Approval ETA-12/0114 – SPAX self-tapping screws*. Copenhagen, Denmark : ETA-Danmark A/S, 2012

[6] KAWRZA, M. ; FURTMÜLLER, T. ; ADAM, C. ; MADEREBNER, R.: Parameter identification for a point-supported cross laminated timber slab based on experimental and numerical modal analysis. In: *European Journal of Wood and Wood Products* vol. 79 (2020), Nr. 2, pp. 317–333. doi: 10.1007/s00107-020-01641-7

[7] LOEBUS, S ; DIETSCH, P. ; WINTER, S: Two-way spanning CLT-concrete-composite slabs. In: *International network on timber engineering research — meeting 50*. Kyoto, Japan, 2017, pp. 263–278

[8] TAPIA, C. ; CLAUS, M. ; AICHER, S.: *Replication Data for: Bond line characteristics of a new screw-glued edge connection for the secondary load-bearing direction of CLT plates*., DaRUS, V1, 2021. doi: 10.18419/darus-2153, UNF:6:dSQ9iue/duvwotJZTCj2XQ==